Doppler effect and cross-section libraries

Alain Hébert

`alain.hebert@polymtl.ca`

Institut de génie nucléaire

École Polytechnique de Montréal

Content (week 5)

- Thermal agitation of nuclides
  - Numerical convolution of the cross sections
  - psi-chi Doppler broadening formulas
- Expansion of the differential cross sections
- Calculation of the probability tables
- ENDF/B evaluations and NJOY processing of cross sections

ENE6101: Week 5

Doppler effect and cross-section libraries – 2/26

1. At energies below 1 eV, there is a continuous exchange of energy between nuclides and neutrons, resulting in a quasi-equilibrium process where a neutron may gain or lose energy.

2. The collision law obtained in Week 3 is no longer valid and a more general relation must be found.

3. This quasi-equilibrium process is affected by the presence of molecular or metallic bindings between nuclides. This binding effect cannot be neglected when the nuclide is used as moderator in the nuclear reactor.

4. The neutron field has no effect on the temperature distribution of the nuclides. Whatever transient or spectral shift experienced by the neutrons, the nuclides remain in thermal equilibrium at absolute temperature T of the material where they live. The velocity distribution of the nuclides is always described by the Maxwell-Boltzmann law.

5. Cross section values are measured and reported in reference tables for a frozen nuclide situation where the material absolute temperature is set at 0K. This situation corresponds to a population of nuclides initially at rest in the LAB, so that the relative velocity V_R of the incident neutron is equal to its real velocity V_n in the LAB.

The element of reaction rate for the reaction x is proportional to the product of the cross section $\sigma_x(V_{\mathrm{R}})$ by the intensity of the beam $I = V_{\mathrm{R}}\, n$, where n is the neutron number density. The cross section is function of $E_{\mathrm{exc}} = \frac{1}{2}\, m V_{\mathrm{R}}^2$. We can write

(1)
$$dR_x \propto V_{\mathrm{R}}\ \sigma_x(V_{\mathrm{R}}) \quad .$$

The velocity distribution $p(\boldsymbol{V}_{\mathrm{A}})$ of the nuclides is the Maxwell-Boltzmann law. The element of reaction rate dR_x is still given by Eq. (1), with the relative velocity now equal to

(2)
$$\boldsymbol{V}_{\mathrm{R}} = \boldsymbol{V}_{\mathrm{n}} - \boldsymbol{V}_{\mathrm{A}} \quad .$$

The average value of $\overline{dR_x}$ for neutrons of velocity V_{n} will be given as

(3)
$$\overline{dR_x} \propto \int_\infty d^3 V_{\mathrm{A}}\ p(\boldsymbol{V}_{\mathrm{A}})\,|\boldsymbol{V}_{\mathrm{n}} - \boldsymbol{V}_{\mathrm{A}}|\ \sigma_x(|\boldsymbol{V}_{\mathrm{n}} - \boldsymbol{V}_{\mathrm{A}}|) \quad .$$

The effects of thermal agitation will be correctly taken into account if we replace "0K" cross sections with averaged values $\overline{\sigma}_x(V_{\mathrm{n}})$ computed in such a way that $\overline{dR_x} \propto V_{\mathrm{n}}\, \overline{\sigma}_x(V_{\mathrm{n}})$.

We obtain an expression for $\overline{\sigma}_x(V_\mathrm{n})$ that is similar to a convolution of the "0K" cross sections by the Maxwell-Boltzmann law:

(4)
$$\overline{\sigma}_x(V_\mathrm{n}) = \frac{1}{V_\mathrm{n}} \int_\infty d^3 V_\mathrm{A}\, p(\boldsymbol{V}_\mathrm{A})\, |\boldsymbol{V}_\mathrm{n} - \boldsymbol{V}_\mathrm{A}|\, \sigma_x(|\boldsymbol{V}_\mathrm{n} - \boldsymbol{V}_\mathrm{A}|) \quad .$$

A remarkable consequence of this relation is that the thermal agitation of nuclides has no effect on a $1/V_\mathrm{R}$ varying cross section. This can be shown by introducing

(5)
$$\sigma_x(V_\mathrm{R}) = \frac{c}{V_\mathrm{R}} \quad ,$$

where c is an arbitrary constant and by substituting this definition in Eq. (4). We obtain

(6)
$$V_\mathrm{n}\, \overline{\sigma}_x(V_\mathrm{n}) = V_\mathrm{R}\, \sigma_x(V_\mathrm{R}) \quad .$$

In general, absorption-type cross sections are not affected by the nuclide agitation at thermal energies of the incident neutron. However, the effects of thermal agitation cannot be neglected in the following cases:

- The application of Eq. (4) on the resonance peaks is at the origin of the Doppler broadening effect. This effect is very important at epithermal energies.

- The thermal agitation of nuclides also has an effect on the direction of the neutron after the collision, so that the collision law obtain in Week 3 is no longer valid. The collision law for the elastic scattering reaction at thermal energies is modified by thermal agitation.

- Finally, the effects of molecular and metallic bindings are creating additional effects on the cross sections and on the collision law. This effect is important at thermal energies and affects the nuclides used as moderator.
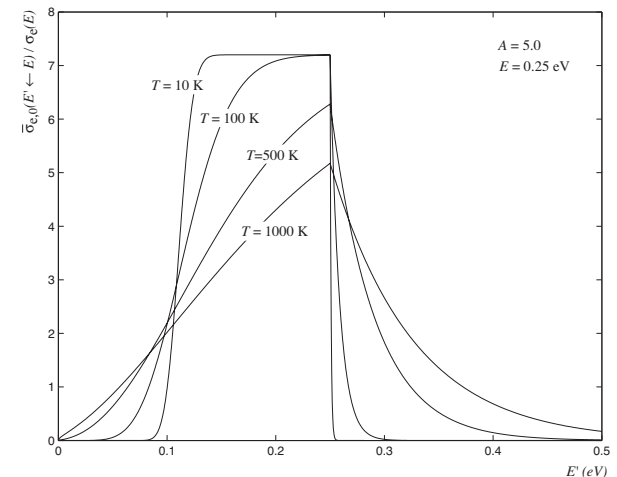
Equation (4) can be partially integrated over $\boldsymbol{V}_A$ without making any approximation. We first introduce the cylindrical coordinate system of he figure, taking care to select the Z–axis in the direction of the incident neutron.
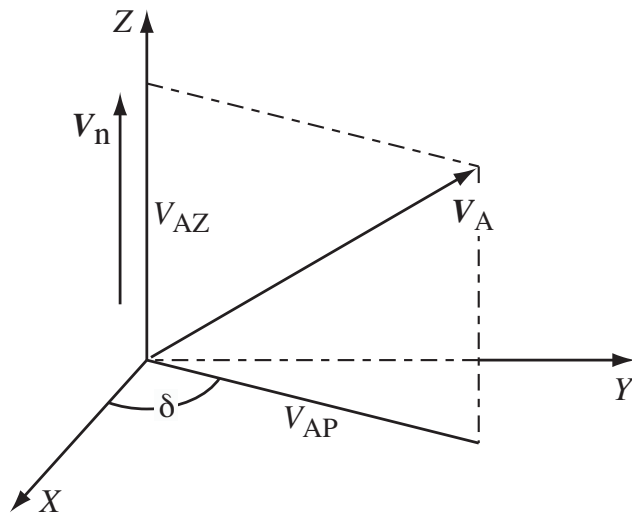
The initial velocity of the nucleus is given as

$$\boldsymbol{V}_A = V_{AP} \cos\delta\, \boldsymbol{i} + V_{AP} \sin\delta\, \boldsymbol{j} + V_{AZ}\, \boldsymbol{k}$$

so that

$$d^3 V_A = V_{AP}\, dV_{AP}\, dV_{AZ}\, d\delta$$

where $-\infty < V_{AZ} < \infty$, $0 \leq \delta \leq 2\pi$ and $0 \leq V_{AP} < \infty$.

Moreover, the squared relative velocity is

$$V_R^2 = |\boldsymbol{V}_n - \boldsymbol{V}_A|^2 = V_{AP}^2 + (V_n - V_{AZ})^2$$

so that

$$V_A^2 = V_R^2 - V_n^2 + 2V_n\, V_{AZ} \ \ .$$

The expression for $\overline{\sigma}_x(V_\mathrm{n})$ is independent of δ. After integration over δ and substitution of the Maxwell-Boltzmann law, Eq. (4) can be written

$$(7) \quad \overline{\sigma}_x(V_\mathrm{n}) = \frac{2\pi}{V_\mathrm{n}} \left(\frac{mA}{2\pi kT} \right)^{\frac{3}{2}} \int_0^\infty dV_\mathrm{AP} \, V_\mathrm{AP} \int_{-\infty}^\infty dV_\mathrm{AZ} \, V_\mathrm{R} \, \exp\left(-\frac{mAV_\mathrm{A}^2}{2kT} \right) \sigma_x(V_\mathrm{R}) \quad .$$

We next perform a change of independent variables, from $\{V_\mathrm{AP}, V_\mathrm{AZ}\}$ toward $\{E_\mathrm{exc}, V_\mathrm{AZ}\}$. We write

$$(8) \qquad E_\mathrm{exc} = \frac{1}{2} m \, V_\mathrm{R}^2 = \frac{1}{2} m \left[V_\mathrm{AP}^2 + (V_\mathrm{n} - V_\mathrm{AZ})^2 \right]$$

and introducing the Jacobian of the transformation, we write

$$(9) \qquad dE_\mathrm{exc} \, dV_\mathrm{AZ} = \begin{vmatrix} \dfrac{\partial E_\mathrm{exc}}{\partial V_\mathrm{AP}} & \dfrac{\partial E_\mathrm{exc}}{\partial V_\mathrm{AZ}} \\[2mm] \dfrac{\partial V_\mathrm{AZ}}{\partial V_\mathrm{AP}} & \dfrac{\partial V_\mathrm{AZ}}{\partial V_\mathrm{AZ}} \end{vmatrix} dV_\mathrm{AP} \, dV_\mathrm{AZ} = m \, V_\mathrm{AP} \, dV_\mathrm{AP} \, dV_\mathrm{AZ} \quad .$$

The support of the distribution after the change of variables is $0 \leq E_\mathrm{exc} < \infty$ and $V_\mathrm{n} - V_\mathrm{R} \leq V_\mathrm{AZ} \leq V_\mathrm{n} + V_\mathrm{R}$.

The change of variables transforms Eq. (7) into

$$
\begin{aligned}
\overline{\sigma}_x(V_{\mathrm{n}}) \; = \; & \frac{2\pi}{V_{\mathrm{n}}} \left(\frac{mA}{2\pi kT} \right)^{\frac{3}{2}} \frac{1}{m} \int_0^\infty dE_{\mathrm{exc}} \sqrt{\frac{2E_{\mathrm{exc}}}{m}} \, \sigma_x(E_{\mathrm{exc}}) \int_{V_{\mathrm{n}}-V_{\mathrm{R}}}^{V_{\mathrm{n}}+V_{\mathrm{R}}} dV_{\mathrm{AZ}} \\
& \times \; \exp\left[-\frac{mA}{2kT} \left(V_{\mathrm{R}}^2 - V_{\mathrm{n}}^2 + 2V_{\mathrm{n}}\,V_{\mathrm{AZ}} \right) \right]
\end{aligned}
$$

(10)

which can be rewritten, after integration in V_{AZ}, as

$$
\begin{aligned}
\overline{\sigma}_x(E) \; = \; & \frac{1}{\Delta\sqrt{\pi}} \int_0^\infty dE_{\mathrm{exc}} \sqrt{\frac{E_{\mathrm{exc}}}{E}} \, \sigma_x(E_{\mathrm{exc}}) \\
& \times \left\{ \exp\left[-\frac{A}{kT} \left(\sqrt{E_{\mathrm{exc}}} - \sqrt{E} \right)^2 \right] - \exp\left[-\frac{A}{kT} \left(\sqrt{E_{\mathrm{exc}}} + \sqrt{E} \right)^2 \right] \right\}
\end{aligned}
$$

(11)

where

(12)
$$
\Delta = 2\sqrt{\frac{EkT}{A}} \quad \text{and} \quad E = \frac{1}{2} m\,V_{\mathrm{n}}^2 \quad .
$$

Equation (11) has been obtained without introducing any additional approximation. A numerical integration in E_{exc} can be used to introduce the effect of thermal agitation on any E_{exc}–dependent cross section, whatever the energy of the incident neutron.

The SLBW formulas can be substituted in Eq. (11). The remaining integration in E_{exc} can be performed analytically, leading to the so-called psi-chi Doppler broadening formulas. Here, we assume that the resonances are narrow, are located above the thermal energy domain and are due to s wave interactions. Under these conditions, we note that

1. The second exponential term in Eq. (11) vanishes, so that

$$\exp\left[-\frac{A}{kT}\left(\sqrt{E_{\mathrm{exc}}}+\sqrt{E}\right)^2\right] \simeq 0 \ .$$

2. The peak energy value E_1 is much greater than the total resonance width Γ_1.

3. We use a Taylor expansion of the first exponential term around E and assume that the first exponential term rapidly vanishes. We set $E_{\mathrm{exc}} = E + \epsilon$, with $\epsilon << E$ and write

$$\left(\sqrt{E_{\mathrm{exc}}}-\sqrt{E}\right)^2 \simeq \frac{(E_{\mathrm{exc}}-E)^2}{4E} \ .$$

4. We assume s wave interaction, so that $\sigma_0(E_{\mathrm{exc}})$ varies as $1/\sqrt{E_{\mathrm{exc}}}$.

5. We assume that $\Gamma_{x,1}$ and Γ_1 are constant.

We remember the SLBW equations for an absorption-type cross section. We write

(13)
$$\sigma_x(E_{\text{exc}}) = \sigma_0(E_{\text{exc}}) \frac{\Gamma_{x,1}}{\Gamma_1} \frac{1}{1 + 4\left[\dfrac{E_{\text{exc}} - E_1}{\Gamma_1}\right]^2} \quad .$$

Moreover, we introduce two reduced variables u and v defined as

(14)
$$u = \frac{2}{\Gamma_1}\left(E - E_1\right) \quad \text{and} \quad v = \frac{2}{\Gamma_1}\left(E_{\text{exc}} - E_1\right)$$

so that Eq. (11) can be rewritten as

(15)
$$\overline{\sigma}_x(E) = \frac{1}{\Delta\sqrt{\pi}}\, \sigma_0(E) \frac{\Gamma_{x,1}}{2} \int_{-2E_1/\Gamma_1}^{\infty} \frac{dv}{1 + v^2}\, \exp\left[-\frac{A}{kT}\frac{\Gamma_1^2\,(v - u)^2}{16E}\right] \quad .$$

The lower integration limit can be replaced by $-\infty$, as $\Gamma_1 << E_1$.

Equation (15) can be simplified by introducing the following parameter:

(16)
$$\beta = \frac{2\Delta}{\Gamma_1} \quad .$$

We obtain

(17)
$$\overline{\sigma}_x(E) = \sigma_0(E) \, \frac{\Gamma_{x,1}}{\Gamma_1} \, \psi(u, \beta)$$

with the Doppler psi function defined as

(18)
$$\psi(u, \beta) = \frac{1}{\beta\sqrt{\pi}} \int_{-\infty}^{\infty} dv \, \frac{1}{1 + v^2} \exp\left[-\frac{(v - u)^2}{\beta^2} \right] \quad .$$

psi-chi Doppler broadening formulas

We now remember the SLBW equation for elastic scattering cross section. We write

$$(19) \quad \sigma_{\mathrm{e}}(E_{\mathrm{exc}}) = 4\pi\,a^2 + \sigma_0\,\frac{2a}{\lambda}\,\frac{2\left[\frac{E_{\mathrm{exc}}-E_1}{\Gamma_1}\right]}{1+4\left[\frac{E_{\mathrm{exc}}-E_1}{\Gamma_1}\right]^2} + \sigma_0\,\frac{\Gamma_{\mathrm{n},1}}{\Gamma_1}\,\frac{1}{1+4\left[\frac{E_{\mathrm{exc}}-E_1}{\Gamma_1}\right]^2}\;.$$

Using the same approximations and the same mathematical treatment, we get the equivalent broadened formula as

$$(20) \quad \overline{\sigma}_{\mathrm{e}}(E) = 4\pi\,a^2 + \sigma_0(E)\,\frac{2a}{\lambda}\,\chi(u,\beta) + \sigma_0(E)\,\frac{\Gamma_{\mathrm{n},1}}{\Gamma_1}\,\psi(u,\beta)$$

with the Doppler chi function defined as

$$(21) \quad \chi(u,\beta) = \frac{1}{\beta\sqrt{\pi}}\int_{-\infty}^{\infty} dv\,\frac{v}{1+v^2}\exp\left[-\frac{(v-u)^2}{\beta^2}\right]\;.$$

We notice that the Doppler broadened Eqs. (17) and (20) reduce to the original SLBW equations as $T \to 0$. In this case, $\beta \to 0$ and

(22)
$$\lim_{\beta \to 0} \psi(u,\beta) = \frac{1}{1+u^2} \quad \text{and} \quad \lim_{\beta \to 0} \chi(u,\beta) = \frac{u}{1+u^2} \ .$$

Simple Matlab scripts can evaluate functions $\psi(u,\beta)$ and $\chi(u,\beta)$ with the help of a ten-point Gauss-Hermite quadrature.

```
function f=psi(beta,x)
% Doppler psi function
  u=[ 3.43615913, 2.53273177, 1.75668371, 1.03661084, 0.342901319, ...
  -0.342901319, -1.03661084, -1.75668371, -2.53273177, -3.43615913 ] ;
  w=[ 7.64043307e-6, 0.00134364574, 0.0338743962, 0.240138605, ...
  0.610862613, 0.610862613, 0.240138605, 0.0338743962, ...
  0.00134364574, 7.64043307e-6 ] ;
  f=0 ;
  for i=1:10
     aaa=1.0./(sqrt(pi)*(1+x.^2+2.*x.*beta.*u(i)+(beta.*u(i)).^2)) ;
     f=f+w(i).*aaa ;
  end
```

psi-chi Doppler broadening formulas 6

However, a more accurate numerical approach consists to evaluate functions $\psi(u,\beta)$ and $\chi(u,\beta)$ with the help of Faddeeva function.

(23) $$\psi(u,\beta) = \frac{\sqrt{\pi}}{\beta}\Re\left[w\left(\frac{u+i}{\beta}\right)\right] \quad \text{and} \quad \chi(u,\beta) = \frac{\sqrt{\pi}}{\beta}\Im\left[w\left(\frac{u+i}{\beta}\right)\right].$$
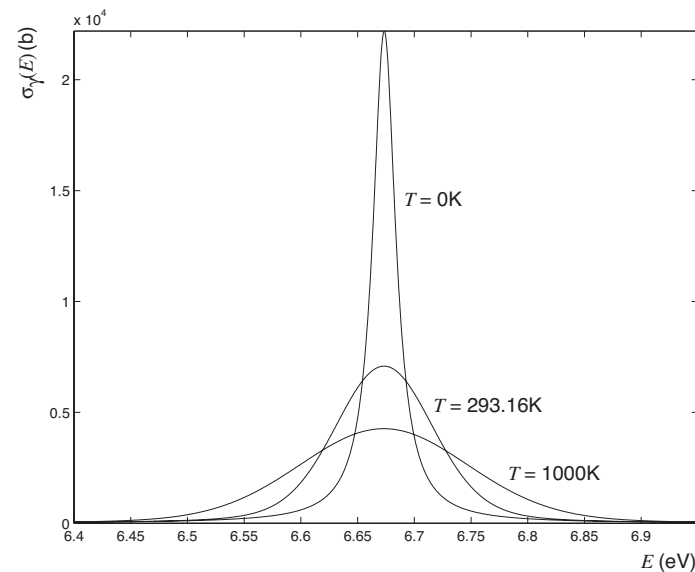
where

(24) $$w(z) = \frac{i}{\pi}\int_{-\infty}^{\infty} dt\, \frac{e^{-t^2}}{z-t}$$

```
function f=psi_voigt(beta,x)
% Doppler psi function in term of Voigt function
% (c) 2015 Alain Hebert, Ecole Polytechnique de Montreal
   Fad_w=@(z) exp(-z^2)*double(erfc(sym(-z*1i)));
   if (beta == 0)
     f=1/(1+x^2);
   else
     f=sqrt(pi)*real(Fad_w((x+1i)/beta))/beta;
   end
```

These formulas can be further simplified by assuming $E \simeq E_1$ in Eq. (12), so that

$$(25) \qquad \beta = \frac{2\Gamma_{\mathrm{D}}}{\Gamma_1} \quad \text{where} \quad \Gamma_{\mathrm{D}} = 2\sqrt{\frac{E_1 kT}{A}} \quad (\text{Doppler width}) \ .$$

The Doppler effect results in a widening of the resonance while preserving the surface under the cross section curve. The higher the temperature of the material, the wider becomes the resonance and the smaller becomes the peak.

Reactor physics calculations generally rely on Legendre expansion of $\sigma_{\mathrm{s}}(E' \leftarrow E, \mu)$ about the deviation cosine μ. We write

$$(26) \qquad \sigma_{\mathrm{s}}(E' \leftarrow E, \mu) = \sum_{\ell=0}^{L} \frac{2\ell + 1}{2} \, \sigma_{\mathrm{s},\ell}(E' \leftarrow E) \, P_\ell(\mu)$$

where L is the scattering order of the collision. $L = 0$ and $L = 1$ correspond to isotropic scattering and to linearly anisotropic scattering in the LAB, respectively. The Legendre components of the differential cross section are

$$(27) \qquad \sigma_{\mathrm{s},\ell}(E' \leftarrow E) = \int_{-1}^{1} d\mu \, \sigma_{\mathrm{s}}(E' \leftarrow E, \mu) \, P_\ell(\mu) \ .$$

Assuming $L = 0$ is generally not acceptable in reactor physics and can only be used in association to a transport correction that will be introduced in next chapter. However, setting $L = 1$ is generally sufficient in reactor physics but may be unacceptable in safety and criticality or in radiation shielding studies.

Probability tables corresponding to the microscopic total cross section $\sigma(u)$ with $u_{g-1} \leq u \leq u_g$ can be defined from the probability density $\Pi(\sigma)$.

$\Pi(\sigma)d\sigma$ is the probability for the microscopic total cross section of the resonant isotope, to have a value between σ and $\sigma + d\sigma$. $\{u_g \; ; \; 1 \leq g \leq N_g + 1\}$ is the multigroup structure containing $N_g + 1$ lethargy limits.
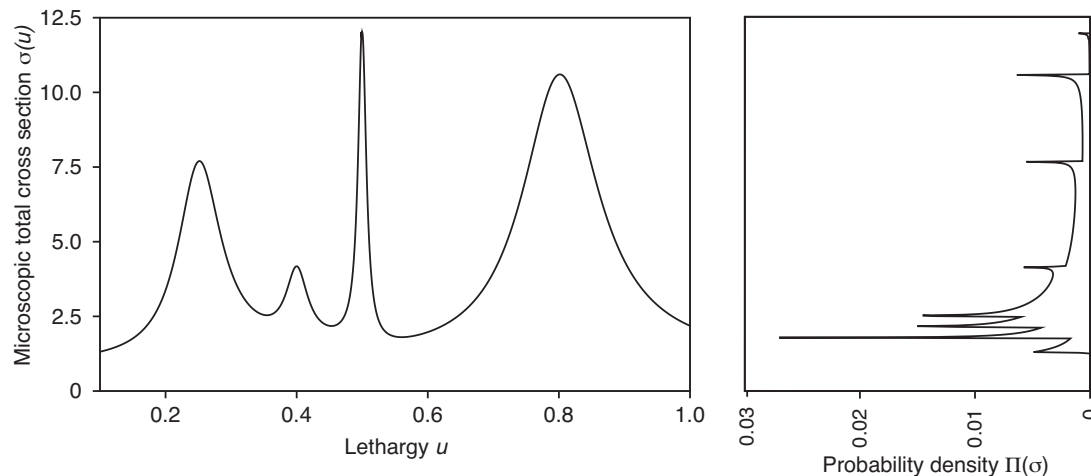
As might be expected, the probability density $\Pi(\sigma)$ is normalized to unity:

(28)
$$\int_0^{\max(\sigma)} d\sigma \, \Pi(\sigma) = 1 \quad .$$

The probability density $\Pi(\sigma)$ is represented by a series of K Dirac distributions centered at discrete values σ_k of the microscopic total cross section for the resonant isotope. Each discrete level is called a subgroup and is also characterized by a discrete weight ω_k. This approach leads to an approximative expression of $\Pi(\sigma)$ written as

(29)
$$\Pi(\sigma) = \sum_{k=1}^{K} \delta(\sigma - \sigma_k)\, \omega_k \quad \text{with} \quad \sum_{k=1}^{K} \omega_k = 1 \quad .$$

Using this definition, any Riemann integral in lethargy, with a σ–dependent integrand, can be replaced by an equivalent Lebesgue integral:

(30)
$$\frac{1}{\Delta u_g} \int_{u_{g-1}}^{u_g} du \, f\left[\sigma(u)\right] = \int_{0}^{\max(\sigma)} d\sigma \, \Pi(\sigma) \, f(\sigma)$$

Substitution of Eq. (27) into Eq. (28) leads to the following discretization:

(31)
$$\frac{1}{\Delta u_g} \int_{u_{g-1}}^{u_g} du \, f\left[\sigma(u)\right] = \sum_{k=1}^{K} \omega_k \, f(\sigma_k) \quad .$$

We can also compute partial cross section information. $\sigma_x(\sigma)$ is the average value of the microscopic partial cross section $\sigma_x(u)$ corresponding to the value $\sigma(u)$ of the total microscopic cross section. The following discretization is used:

(32)
$$\Pi(\sigma)\,\sigma_x(\sigma) = \sum_{k=1}^{K} \delta(\sigma - \sigma_k)\,\sigma_{x,k}\,\omega_k \quad .$$

Partial cross section information can also be used to discretize the Riemann integral:

(33)
$$\frac{1}{\Delta u_g} \int_{u_{g-1}}^{u_g} du\,\sigma_x(u)\,f\left[\sigma(u)\right] = \sum_{k=1}^{K} \omega_k\,\sigma_{x,k}\,f(\sigma_k) \quad .$$

The set of values $\{\omega_k,\,\sigma_k,\,\sigma_{x,k}\,;\; k=1,K\}$ corresponding to energy group g is the probability table describing the resonant behavior of the cross sections.

1. Levitt introduced the term probability table to describe a quadrature set in which the base points in cross section are fixed a priori. The terms subgroup and multiband were introduced by Nikolaev and Cullen, respectively, to describe a quadrature set in which the base point and weights are simultaneously computed.

2. The CALENDF approach of Ribon is therefore an outgrowth of the techniques introduced by these two authors. In the following text, we will use the terminology proposed by Ribon. A probability table will be view as a quadrature set representing a probability density with a set of Dirac delta distributions.

3. The term subgroup equation will be used to represent a transport equation in which some probability densities are replaced with probability tables.

4. The moment approach consists to compute the probability table by solving the non-linear system obtained by setting $f[\sigma(u)] = \sigma(u)^\ell$ with $L_{\min} \leq \ell \leq L_{\max}$ in Eq. (29). The base points for the partial cross section x are obtained by setting $f[\sigma(u)] = \sigma(u)^\ell$ in Eq. (31), using the weights of Eq. (29).

5. The CALENDF probability tables are consistent. The base points are constrained as follows: $\min(\sigma(u)) \leq \sigma_k \leq \max(\sigma(u))$; the values of the probability table are real, the weights are positive, and their sum is equal to one.
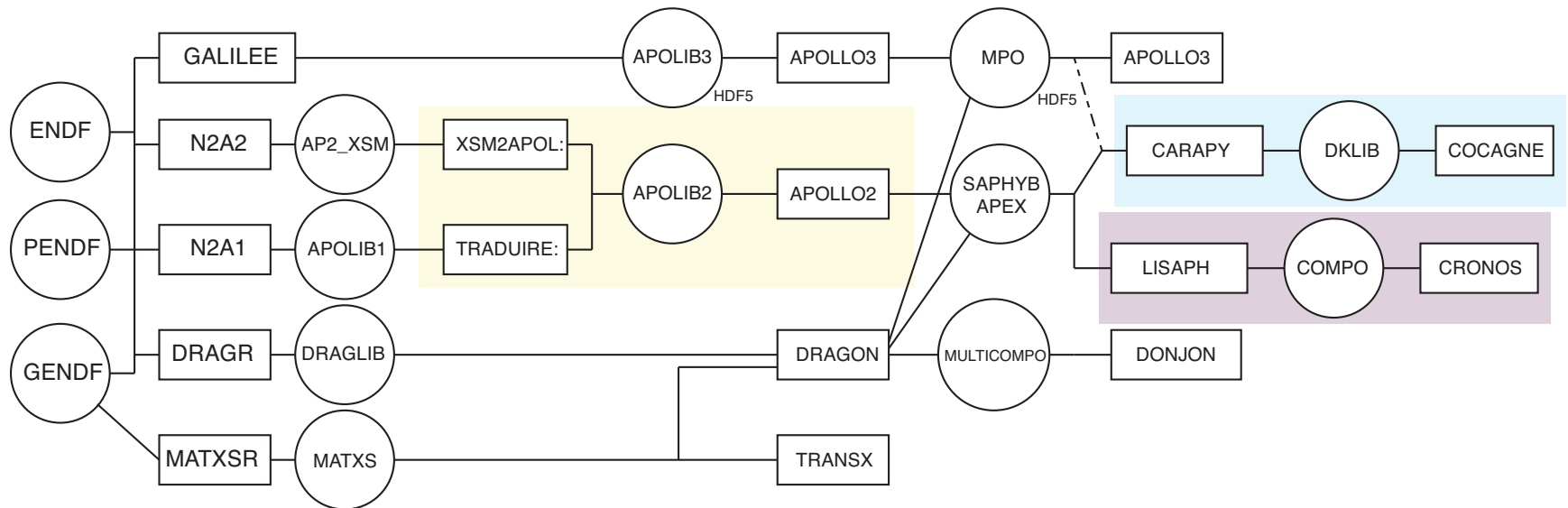
Each isotope of the evaluation is processed into a specific NJOY data flow, in order to produce an isotopic cross-section library consistent with the type of transport equation solution. The corresponding data flow is depicted in the figure:
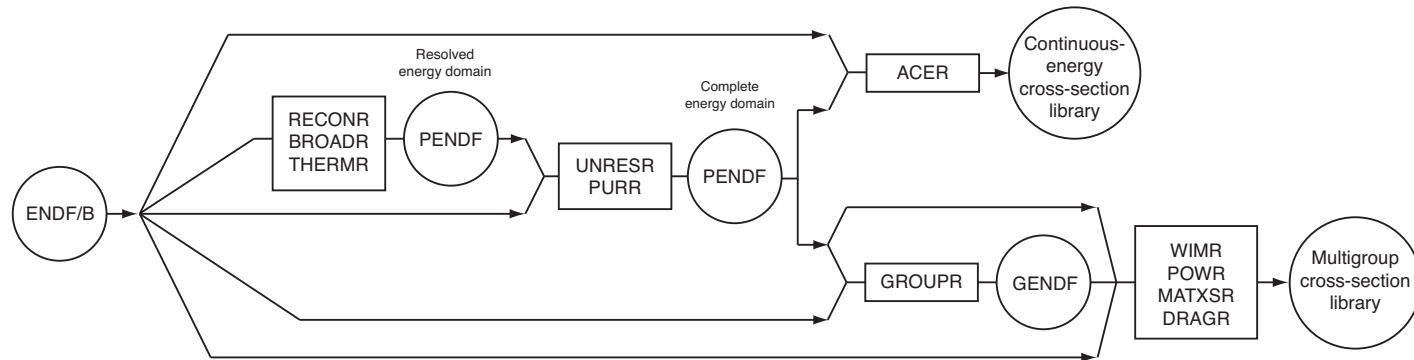
RECONR: resonance reconstruction at 0K

BROADR: numerical convolution for Doppler effect

THERMR: $S(\alpha, \beta)$ model, including free gas model

UNRESR: compute self-shielded cross sections at unresolved energies

PURR: same as UNRESR and compute probability tables at unresolved energies

ACER: creation of a continuous-energy cross-section library in ACE format

GROUPR: multigroup formatting of cross sections

DRAGR :   creation of a multigroup cross-section library in Draglib format

MATXSR :   creation of a multigroup cross-section library in MATXS format

- At the end of the NJOY calculation, cross section and other nuclear data is formatted into multigroup cross-section libraries to be used in specific lattice codes
  - Lattices codes: APOLLO2, APOLLO3, DRAGON
- Lattice codes are producing specific multi-parameter reactor databases to be used in specific full-core simulation codes
  - Full-core simulation codes: APOLLO3, COCAGNE, CRONOS, DONJON

```
                                                                          1
9.223800+4 2.360058+2          1          1          0      59237
0.000000+0 1.000000+0          0          0          0      69237
1.000000+0 3.000000+7          6          0         10      79237
0.000000+0 0.000000+0          0          0        675    1179237
 92-U -238 ORNL,LANL+ EVAL-SEP06 Young,Chadwick,Derrien,Courcelle 9237
                     DIST-DEC06 REV2-                              9237
----ENDF/B-VII       MATERIAL 9237          REVISION 2            9237
-----INCIDENT NEUTRON DATA                                        9237
------ENDF-6 FORMAT                                               9237
***************************************************************** 9237
                                                                  9237
             ENDF/B-VII EVALUATION                                9237
                                                                  9237
P.G.Young, M.B.Chadwick, R.E.MacFarlane, W.B.Wilson, D.G.Madland, 9237
            P.Talou, T. Kawano (LANL)                             9237
                      and                                         9237
  H. Derrien, A. Courcelle, L. C. Leal, N. Larson (ORNL)          9237
...
```

```
...
 0.000000+0 0.000000+0                  0                  0                  0               09237
 9.223800+4 2.360058+2                  0                  0                  1               09237
 9.223800+4 1.000000+0                  0                  0                  2               09237
 1.000000-5 2.000000+4                  1                  3                  0               09237
 0.000000+0 9.480000-1                  0                  0                  2               29237
 2.360060+2 9.480000-1                  0                  0               5556            9269237
-9.330000+1 5.000000-1 7.658435-3 2.300000-2 0.000000+0 0.000000+09237
-7.330000+1 5.000000-1 5.086118-3 2.300000-2 0.000000+0 0.000000+09237
-5.330000+1 5.000000-1 2.932955-3 2.300000-2 0.000000+0 0.000000+09237
-3.330000+1 5.000000-1 1.004548-2 2.300000-2 2.010000-6 0.000000+09237
-7.000000+0 5.000000-1 1.685000-4 2.300000-2 0.000000+0 0.000000+09237
 6.673491+0 5.000000-1 1.475792-3 2.300000-2 0.000000+0 9.990000-99237
 2.087152+1 5.000000-1 1.009376-2 2.286379-2 5.420000-8 0.000000+09237
 3.668212+1 5.000000-1 3.354568-2 2.300225-2 0.000000+0 9.770000-99237
 6.603118+1 5.000000-1 2.417823-2 2.330763-2 5.265000-8 0.000000+09237
 8.074744+1 5.000000-1 1.873989-3 2.338714-2 0.000000+0 6.049000-89237
...
```